Biological length scale topography enhances cell-substratum adhesion of human corneal epithelial cells

Nancy W. Karuri[1], Sara Liliensiek[2], Ana I. Teixeira[1], George Abrams[2], Sean Campbell[2], Paul F. Nealey[1,*,‡] and Christopher J. Murphy[2,*,‡]

[1]Department of Chemical Engineering, and [2]Department of Surgical Sciences, School of Veterinary Medicine, University of Wisconsin, Madison, WI 53706, USA

*Authors contributed equally to this work

‡Authors for correspondence (e-mail: nealey@engr.wisc.edu; murphyc@svm.vetmed.wisc.edu)

Accepted 9 February 2004
Journal of Cell Science 117, 3153-3164 Published by The Company of Biologists 2004
doi:10.1242/jcs.01146

Summary

The basement membrane possesses a rich 3-dimensional nanoscale topography that provides a physical stimulus, which may modulate cell-substratum adhesion. We have investigated the strength of cell-substratum adhesion on nanoscale topographic features of a similar scale to that of the native basement membrane. SV40 human corneal epithelial cells were challenged by well-defined fluid shear, and cell detachment was monitored. We created silicon substrata with uniform grooves and ridges having pitch dimensions of 400-4000 nm using X-ray lithography. F-actin labeling of cells that had been incubated for 24 hours revealed that the percentage of aligned and elongated cells on the patterned surfaces was the same regardless of pitch dimension. In contrast, at the highest fluid shear, a biphasic trend in cell adhesion was observed with cells being most adherent to the smaller features. The 400 nm pitch had the highest percentage of adherent cells at the end of the adhesion assay. The effect of substratum topography was lost for the largest features evaluated, the 4000 nm pitch. Qualitative and quantitative analyses of the cells during and after flow indicated that the aligned and elongated cells on the 400 nm pitch were more tightly adhered compared to aligned cells on the larger patterns. Selected experiments with primary cultured human corneal epithelial cells produced similar results to the SV40 human corneal epithelial cells. These findings have relevance to interpretation of cell-biomaterial interactions in tissue engineering and prosthetic design.

Key words: Nanoscale topography, Cell-substratum adhesion, Epithelium

Introduction

The extracellular matrix (ECM) provides support for cells and creates an environment where cells can interact with their surroundings. The ECM has been reported to influence cell shape, differentiation and growth (Abrams et al., 2002b; Flemming et al., 1999; Timpl, 1996; Timpl, 1989). All epithelial cells rest upon a specialized form of the ECM, known as the basement membrane. Basement membranes have been reported to consist of filaments composed of collagen, laminin, proteoglycans and other fibrils which form a complex nanometer sized topography of pores, fibers and ridges (Abrams et al., 2002a; Abrams et al., 2000a; Abrams et al., 2000b). In addition to providing chemical stimuli, basement membranes possess a rich three-dimensional surface topography that presents biophysical cues to the overlying cells. Although the components and topography of basement membranes of various epithelial tissues have been characterized, the mechanisms involved in influencing cell behavior, such as adhesion and migration, are not well understood (Curtis and Wilkinson, 1997).

Cell alignment and migration in response to micron and nano sized grooved substrata, contact guidance, has been observed in many different cell types including epithelial cells derived from porcine periodontal ligament explants, explants from human gingival fibroblasts, human corneal epithelial cells and central nervous system neurites (Abrams et al., 2002b; Brunette, 1986a; Brunette, 1986b; Flemming et al., 1999; Rajnicek et al., 1997; Rajnicek and McCaig, 1997; Teixeira et al., 2003). While the relationship between contact guidance and cell-substratum adhesion has not been established, it has been reported that the subpopulations of aligned and elongated fibroblasts on microscale grooves have a higher production of the adhesive protein fibronectin as compared to nonaligned cells (Chou et al., 1995). Recently, contact guidance has been observed for corneal epithelial cells on uniform nanoscale grooves and ridges (Teixeira et al., 2003). Teixeira and co-workers also reported that focal adhesions formed on the patterned nano- and microscale substrata. They also showed that the morphologic characteristics of focal adhesions and their orientation relative to the topographic features were directly influenced by the sizes of the features and the culture environment. Focal adhesions are associated with strong cell-matrix associations (Woods and Couchman, 1988).

On the basis of the above observations, we hypothesized that biological length scale topographic features have the greatest impact in modulating fundamental cell behaviors including cell-substratum adhesion. Interestingly, while there have been a number of studies that have investigated the adhesion of sheets of cells on biologically relevant substrata (Evans et al., 1999b; Evans et al., 2003), we know of no previous studies to quantify the strength of cell-substratum adhesion of single cells

on topography with dimensions that model that of the native basement membrane.

Thus, the aim of this study was to perform a quantitative analysis of the adhesion of human corneal epithelial cells on planar, nano- and microscale grooved substrata. X-ray lithography was used to fabricate silicon substrata with uniform grooves and ridges ranging from 400-4000 nm pitch. Another unique aspect of this study is that through careful substratum design and fabrication we produced single silicon chips containing a range of topographies, from nano- to microscale, that provides a better statistical assessment in the cell experiments. These substrata also facilitate in the search for transitions in cell behavior as features decrease from micro- to nanoscale dimensions. The fact that the differing topographies reside in a single small chip decreases the probability of introducing confounding variables associated with small variations in the cells used and culture conditions in which the experiments were conducted. An SV40 transformed human corneal epithelial cell line [SV40-HCECs (Araki-Sasaki et al., 1995)] was used as a model for corneal cell adhesion in vivo. SV40-HCECs have been reported to exhibit similar growth and differentiation characteristics as primary cells, and to be non-tumorigenic (Araki-Sasaki et al., 1995). The strength of cell-substratum adhesion was examined with the use of a flow cell chamber. The flow cell chamber produces well-defined shear forces and is able to mimic forces imparted to corneal epithelial cells by the motion of blinking (King-Smith et al., 2000; Fatt, 1992).

In his review of the architectural basis of cellular mechanotransduction, Ingber proposed that the way in which the cell cytoskeleton is organized will itself alter the way in which the cell senses and responds to stresses (Ingber, 1997). To investigate the possible interplay between shear forces generated by flow and surface topography in modulating cell adhesion, we analyzed the morphology of cells before and after exposure to shear forces induced by laminar fluid flow. We report here that biologic length scale topographic features profoundly impact cell-substratum adhesion.

Materials and Methods

Preparation of nanoscale patterns

Silicon wafers were patterned with uniform grooves and ridges using X-ray lithography. The wafer surfaces were cleaned and primed with hexamethyldisilazane (Yield Engineering Systems, San Jose, Ca, USA) in a vacuum oven. UV6 photoresist (Shipley, Malborough, Ma, USA) was spin-coated in a resist spinner (Solitec Wafer Processing, Inc., San Jose, Ca, USA) onto the silicon surfaces at rotation speeds of 2000-4000 rpm to produce films 0.3-0.5 μm thick. The coated surfaces were baked at 130°C for 90 seconds to remove residual solvent from the polymer film and relax stresses. The photo resist was patterned on an X-ray Suss XRS-200/2M Stepper (Center for Nanotechnology, University of Wisconsin-Madison, USA). Patterning was done by bringing the photo resist 25-30 μm away from an X-ray mask and exposing it through the mask. A post exposure bake was performed on the resist by heating at 130°C for 60 seconds on a hot plate. The exposed and baked films were then immersed in developing solution (MF320, Shipley, Marlborough, MA) for 60 seconds and rinsed in deionized water.

After resist patterning, reactive ion etching with a Helicon Etching tool (Center for Plasma Aided Manufacturing, University of Wisconsin-Madison, USA) was used to create the three dimensional nanoscopic features on the silicon surfaces. SF_6 and $C_2H_2F_4$ gases both at a flow rate of 18 sccm were used to selectively etch the silicon wafers. The gas pressure was 2 mTorr and the antenna power was 1.5 kW. The power applied to the wafer chuck was 15 W, which corresponded to a bias voltage of –35 V. The antenna discharge, as well as the wafer chuck, was pulsed at a frequency of 33.3 kHz with 50% duty cycle. After etching, the remaining resist was removed by submerging the wafers in piranha solution (70% vol H_2SO_4, 30% vol H_2O_2) at 110°C for 30 minutes and rinsing repeatedly with deionized water.

To ensure uniform surface chemistry, a layer of silicon oxide, approximately 2 nm thick, was deposited on the wafers in a Low Pressure Chemical Vapor Deposition Reactor (LPCVD, University of Wisconsin-Madison). The wafers were then cut into rectangles measuring 60 mm×35 mm with a diamond saw (MicroAutomation 1006, Woodcliff Lake, NJ, USA). The size of the substrata corresponded to the size of the flow cell chamber. Before plating cells, the surfaces were rinsed 2×10 minutes in deionized water and 2×10 minutes in ethanol (Aaper Alcohol and Chemical Co., Shelbyville, KY, USA). The surfaces were then air dried in a laminar flow hood for 20 minutes prior to cell plating.

Surface characterization

Scanning electron microscopy (SEM) and atomic force microscopy (AFM) were used to characterize substrata. A LEO 1530 electron microscope (Leo Electron Microscopy Inc., Thornwood, NY, USA) operating at 5 kV and integrated with image analysis software was used to characterize the surfaces. In addition, a Topometrix Explorer SPM (Center for Nanotechnology, University of Wisconsin-Madison) equipped with carbon nanotube tips (Piezomax Technologies, Madison, WI, USA) in intermittent-contact mode was used to verify SEM measurements. The dimensions examined included the ridge and groove width and the depth of the groove structures (Fig. 1). The pitch, which is the periodicity of the structures, was used to define the topographical area. For surface characterization, the experiment had two factors: feature size and the different substrata used. Feature size had seven levels: the 400, 800, 1200, 1600, 2000 and 4000 nm pitch dimensions and the planar surface. The planar surface was used as a control for comparison of cell attachment to patterned surfaces. A total of five substrata were used.

Cell culture

SV40-HCECs [from Dr Kaoru Araki-Sasaki, Kiniki Central Hospital, Hyogo, Japan (Araki-Sasaki et al., 1995)] were grown to 90-95% confluence in 75 cm^2 culture flasks at 35°C with 5% CO_2 in a modified, Supplemented Hormonal Epithelial Medium (SHEM; Sigma-Aldrich, Co., St Louis, MO, USA). SHEM, which is made up of Dulbecco's modified Eagle's medium (DMEM), Ham's F-12, plus 0.5% dimethyl sulfoxide and 40 μg/ml of gentamycin was supplemented with 10% fetal bovine serum (FBS; Sigma-Aldrich, Co.). Passages 29-34 of the SV40-HCECs were used for our experiments. After achieving the desired confluence, the cells were passaged using 0.025% trypsin/0.01% EDTA for 10 minutes at 37°C and 5% CO_2. Trypsin was then inactivated by the addition of FBS. The cells were centrifuged for 3 minutes and then resuspended in 10 ml of SHEM medium. Selected experiments were repeated with primary cultured HCECs using previously published methods (Teixeira et al., 2003).

Adhesion assay

SV40-HCECs were seeded to each substratum containing the seven different topographical areas: planar, 400 nm pitch, 800 nm pitch 1200 nm pitch, 1600 nm pitch, 2000 nm pitch and 4000 nm pitch. Cells were seeded at a concentration of 4.5×10^4 cells/ml in 10 ml of SHEM medium on each substratum in a 90 mm diameter Petri dish. This cell

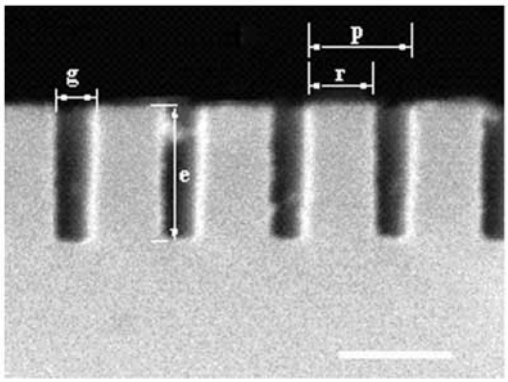

Fig. 1. Characterization of nanostructured surfaces. Scanning electron microscopy image of a cross-sectional view of the silicon structures created by X-ray lithography. p, pitch; g, groove size; r, ridge size; e, etch depth. Scale bar: 400 nm.

seeding density was found to be the optimal for ensuring maximum surface coverage and minimum cell-cell contact formation. The plated cells were then incubated (37°C, 5% CO_2) for 24 hours. Preliminary experiments had indicated that a 24-hour incubation period was necessary to ensure optimal cell attachment to the substrata.

Following incubation, cell adhesion was evaluated using a flow cell chamber (Fig. 2A). The flow cell had dimensions of 40×14×0.16 mm^3 [length (l) × width (w) × height (h)]. For one-dimensional laminar flow, the wall shear stress τ_w is given as in Bird et al. (Bird et al., 1960):

$$\tau_w = \frac{6\mu Q}{wh^2} \quad (1)$$

where μ is the fluid viscosity and Q is the volumetric flow rate. At the maximum volumetric flow rate used, 4.64 ml/second, the entrance length was found be less than 5% of the chamber length allowing for uniform laminar flow over the entire length of the chamber (Bird et al., 1960).

Two distinct sets of testing conditions were used to examine cell adhesion. In the first set of conditions, after incubation, cells were subjected to steps of increasing shear force (Fig. 2B). During the course of the assay, cells on each of the seven different topographical areas on the substratum were viewed and imaged using a Zeiss Axiovert 200/200M microscope (Carl Zeiss Microimaging, Thornwood, NY, USA). The area of analysis was located at the center of the flow cell chamber. Before the onset of flow, the computer driven stage was used to place the center of the patterned region under the microscope lens. The stage position was saved and an image of the cells in this region was captured. A 10× objective and a 1.00× optovar corresponded to an image area of 1.34 mm^2 and a cell count of 35-45 cells. Using the memorized positions, an image of the cells was taken every 5 minutes, immediately prior to each increase in fluid shear. In the second set of conditions, after incubation, adherent cells were exposed to a constant shear stress of 10 Pa for 15 minutes and then fixed. The total number of adherent cells on each patterned region was then determined.

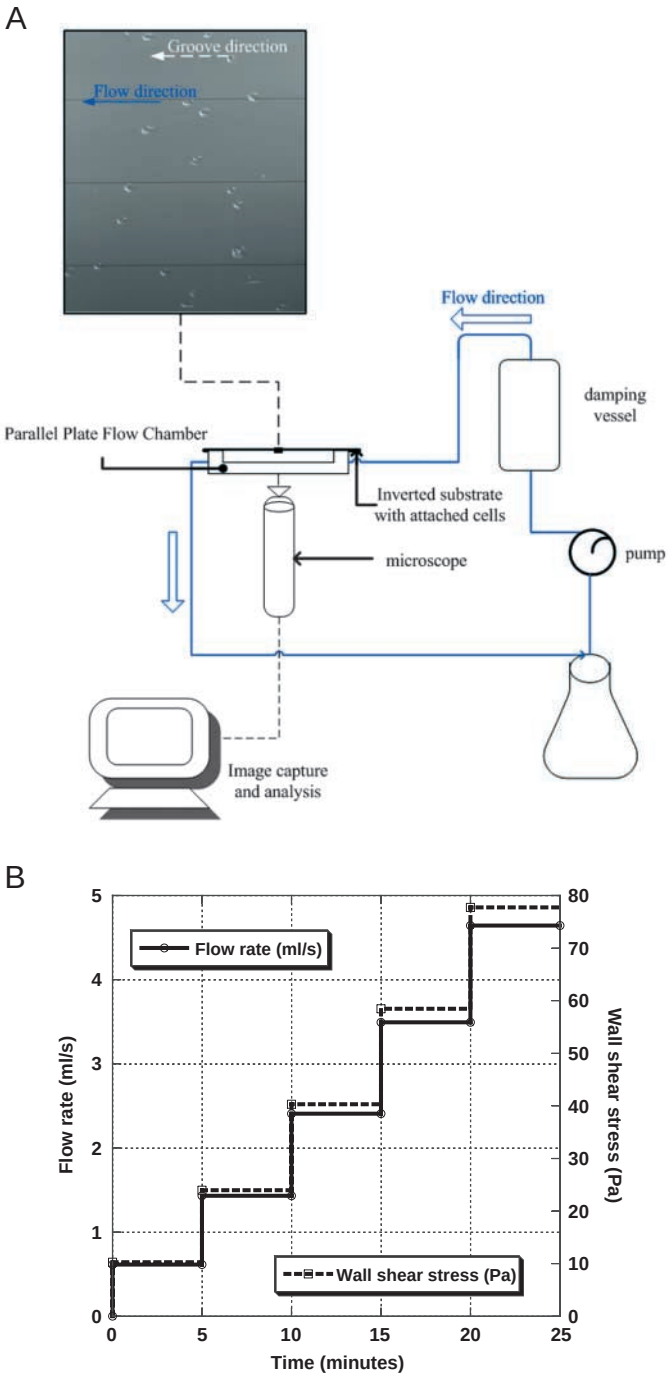

Fig. 2. (A) Schematic of flow cell and image capture and analysis system. Fluid is circulated by the peristaltic pump, through the damping vessel and into the parallel plate flow chamber to yield uniform shear on the substratum. The damping vessel serves to reduce pulsatile flow. (B) Profile of the calculated volumetric flow and associated wall shear stress that cells were exposed to. The circulating fluid for this profile was DPBS solution.

Effect of shear stress on cell morphology

To investigate the possible relationship between cell morphology and cell adhesion, we quantified the number of aligned and elongated cells before and after flow. We used analytic techniques similar to those of Teixeira and co-workers (Teixeira et al., 2003) to determine the total number of adherent cells and cell morphology both after the 24-hour incubation period and at the end of the adhesion assay. F-actin in SV40-HCECs was labeled with fluorescently tagged phalloidin. The cells were then rinsed with Dulbecco's phosphate-buffered saline (DPBS; BioWhitaker, Walkersville, MD) and fixed in 4% paraformaldehyde (Electron Microscopy Sciences, Washington, PA, USA), 5% sucrose in 10 mM phosphate buffered solution (pH 7.4) at

room temperature for 20 minutes. The cells were then permeabilized with 0.1% Triton X-100 (Sigma-Aldrich, Co.) in DPBS for 5 minutes and blocked with 1% bovine serum albumin (Sigma-Aldrich, Co.) in DPBS for 20 minutes. Actin filaments were labeled by incubating the cells with 5 μg/ml of TRITC-phalloidin (Molecular Probes, Inc., Eugene, OR) in DPBS for 30 minutes. The cells were then rinsed 3×10 minutes in DPBS. After rinsing, the cells were incubated in 0.3 μM 4′,6-diamidino-2-phenylindole (DAPI; Molecular Probes, Inc.) in DPBS for 10 minutes to stain the nuclei. The substrata were then coated with Antifade (ProLong Antifade Kit, Molecular Probes) and covered with a glass coverslip.

The fixed and stained cells were imaged and analyzed for number, orientation, elongation and projected area using fluorescence microscopy (Carl Zeiss Ltd). An area of 4 mm^2 was examined for each topographical area. KS image analysis software (Carl Zeiss Ltd) was used to evaluate the orientation angle, major and minor axes and pixilated area of individual cells (Teixeira et al., 2003). Cells were considered aligned if the orientation angle $\leqslant 10°$. Cell elongation was characterized by an elliptical form factor, which is calculated as the length of a cell divided by its width. Cells were considered elongated if the elliptical form factor $\geqslant 1.3$. Assuming position on the surface did not affect cell morphology we obtained replicates by determining the percentage at different positions on a specific topographical area.

To ensure that the force felt by the cells was essentially the same for all feature sizes we sought to determine the cell-substratum contact area and the thickness of the cell. SEM analysis was performed on SV40-HCECs incubated for 24 hours on the seven patterned areas. In brief, the cells were rinsed in 0.1 M cacodylate buffer for 10 minutes and fixed in 3% glutaraldehyde in cacodylate buffer (Tousimis Corp., Rockville, MD) for 2.5 hours. Following fixation, the cells were rinsed in cacodylate buffer and post-fixed in 1% osmium tetroxide (Tousimis Corporation) for 1 hour. Subsequently, the cells were dehydrated in graded ethanol (70-100 vol%) and immersed in hexamethyldisilazane for 10 minutes. Finally, the cells were coated with 2 nm of platinum and imaged using SEM.

Cell thickness prior to the adhesion assay was assessed by DiI membrane labeling and fluorescence confocal microscopy. After incubation cells were rinsed 2×10 minutes in DPBS. The cells were then incubated in 1 μg/ml DiI solution (1,1′-dioctadecyl-3,3,3′,3′-tetramethylindocarbocyanine perchlorate; Molecular Probes) for 5 minutes at 37°C, 5% CO_2 and then incubated at 4°C for 15 minutes. Following incubation, the cells were rinsed for 3×10 minutes in DPBS, mounted with Antifade (Molecular Probes) and examined using a confocal microscope (Bio-Rad MRC-1024 laser scanning confocal microscope; Bio-Rad Laboratories, Hercules, CA, USA). The thickness of the cell was measured by focusing on the apical membrane and the basal membrane and then subtracting the basal from the apical z-distance.

Statistical analysis

A two-way ANOVA test was used to reveal whether any of the experimental groups were affected by topography and wall shear stress and also to examine possible interactions between flow and topography in modulating cellular responses. A statistical analysis using Student's *t*-test was performed in cases where experiments were carried out at least in triplicate. A level of $P=0.05$ was accepted as statistically significant.

Results

Surface characterization

We observed uniform grooves and ridges across the entire patterned regions. A representative SEM cross sectional view of the patterned surfaces together with characteristic feature dimensions are shown in Fig. 1. A summary of measurements of the five different substrata taken by SEM and AFM is shown in Table 1. The variability between the groove and ridge sizes on our patterns is probably due to the quality of the mask structure. Our measurements indicated that etch depth varied with pitch size. An increase in pitch size from 400 to 4000 nm correlated with an increase in groove depth, from approximately 250 nm to 600 nm. We assumed that the differences in groove depth between the substrata were not significant in subsequent cell assays. Therefore, our measurements confirmed expected fabrication specifications for substrata to be used in subsequent assays.

Table 1. Average surface dimensions of the nanostructured surfaces

Surface	Ridge size (r), nm	Groove size (g), nm
400 nm pitch	222±21	176±19
800 nm pitch	453±18	344±18
1200 nm pitch	680±52	511±54
1600 nm pitch	932±31	664±29
2000 nm pitch	1133±26	863±36
4000 nm pitch	2150±57	1835±51

The average depth (e) was approximately 400±150 nm; owing to diffusion limitations in the etching process, the large pitches had higher depth values. Mean±s.e.m. $n=5$.

Effect of substratum topography and fluid flow on cell morphology and adhesion

F-actin staining revealed morphologic changes in SV40-HCECs associated with the presence of a patterned substratum. Analysis of our results indicated 35-45% of SV40-HCECs aligned and elongated (orientation angle $\leqslant 10°$ and elliptical form factor $\geqslant 1.3$) in the direction of the grooves of each of the patterned surfaces (data not shown). In contrast, cells on the planar surface were rounded and the percentage of aligned and elongated cells on this surface was below 5%. There was no significant difference ($P\leqslant 0.05$) detected in the numbers of cells aligned and elongated among the different pitch dimensions on each substratum. In agreement with the findings of Teixeira and co-workers, aligned and elongated cells on both the planar and patterned surfaces were found to have on average a higher projected area than the cells with a more rounded morphology (Teixeira et al., 2003) (data not shown).

Morphological changes related to substratum topography detected by fluorescence microscopy were confirmed by SEM analysis. Fig. 3 shows images of fixed SV40-HCECs on the planar surface (Fig. 3A) and on the 400 and 4000 nm pitches (Fig. 3B). Cross-sectional SEM analysis revealed that cell-substratum contacts were restricted to the tops of the ridges. However, the presence of filopodia and lamellipodia in the grooves and ridges of the patterned surfaces (Fig. 3C) were observed at the cell periphery of the leading and rear edge of aligned and elongated cells. This is consistent with published work from our laboratories investigating primary corneal epithelial cell behavior on similar surfaces (Teixeira et al., 2003). Confocal microscopic studies revealed, on average, cell thickness was not statistically different among the seven topographical areas ($0.5\leqslant P\leqslant 0.80$). The mean thickness of SV40-HCECs on all the topographical areas was 6.2±0.05 μm. Subsequently, SEM and confocal microscopy revealed that the

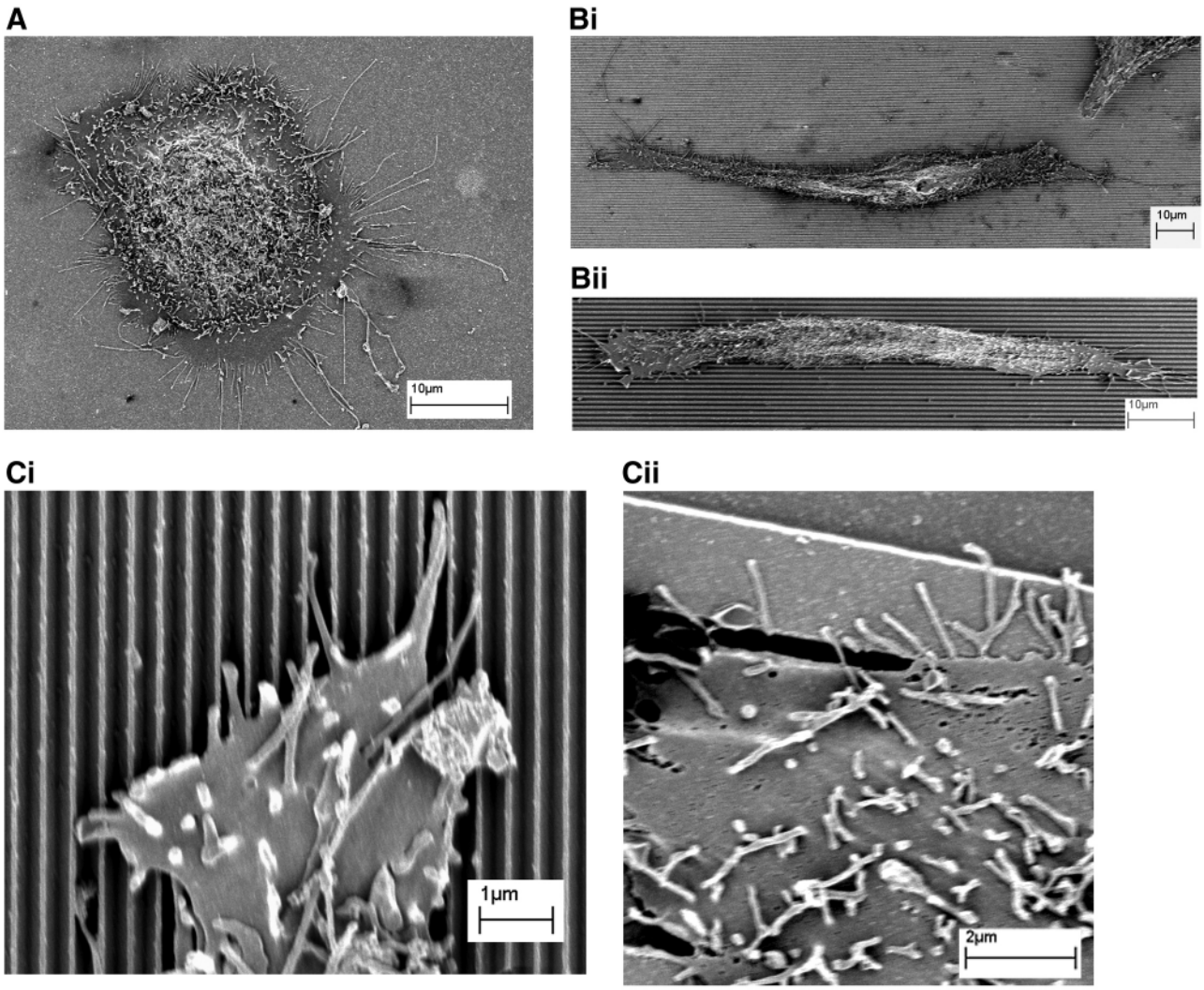

Fig. 3. SEM images of adherent SV40-HCECs on the surfaces. (A) Planar surface. (B) Patterned surfaces: (i) 400 nm pitch, (ii) 4000 nm pitch. (C) Tip of an elongated cell: (i) 400 nm pitch, (ii) 4000 nm pitch.

cell-substratum contact area and the cell thickness were essentially the same for all patterned feature sizes and planar surfaces.

Substratum topography led to changes in cell-substratum adhesion after 24 hours of incubation. Fig. 4 presents images of cells before and after exposure to fluid shear. Images of the populations of SV40-HCECs taken before flow (Fig. 4A,C,E) and during maximum flow (Fig. 4B,D,F) show a decrease in the number of attached cells in response to the applied force. We also observed that the number of detached cells was dependent on the surface topography. We did not observe cellular debris or 'ghost cells' usually associated with cohesive failure of the cell due to the applied force (Richards et al., 1995). The most dramatic difference in cell attachment after maximum flow was between the 400 nm pitch and the planar surfaces (Fig. 4B,F) and between the 400 and 4000 nm pitch surfaces (Fig. 4B,D).

A quantitative analysis of cell detachment as a function of wall shear stress confirmed these initial findings. The percentages of adherent cells in response to the fluid shear profile in Fig. 2B on the different topographical areas are illustrated in Fig. 5. The numbers were calculated from the average of four patterned and planar regions. For clarity, only the planar, 400 nm pitch, 1200 nm pitch, 2000 nm pitch and 4000 nm pitch are represented in Fig. 5A,i. Differences in cell attachment were most pronounced at the highest wall shear stress. Cell attachment at the highest wall shear stress was suggestive of a biphasic response to pattern feature sizes (Fig. 5Aii). At substratum pitch less or equal to 1200 nm, a much greater cell adhesive response to the applied fluid shear was observed as compared to a pitch size equal to or greater than 1600 nm. On the 400 nm pitch surface, at a wall shear stress of 80 Pa, 66% of the initial cell population remained attached, which was significantly higher than the attachment on the 1600 nm pitch surface (38% cell attachment, P=0.008), the 2000 nm pitch surface (39% cell attachment, P=0.002), the 4000 nm pitch surface (41% attachment, P=0.041) and the planar surface (38% cell attachment, P=0.005). At each of the wall shear stresses sampled, the planar surface was statistically indistinguishable from the 4000 nm pitch ($0.25 \leqslant P \leqslant 0.81$).

The same trends in cell detachment were observed for cells undergoing continuous fluid shear (10 Pa) in SHEM medium

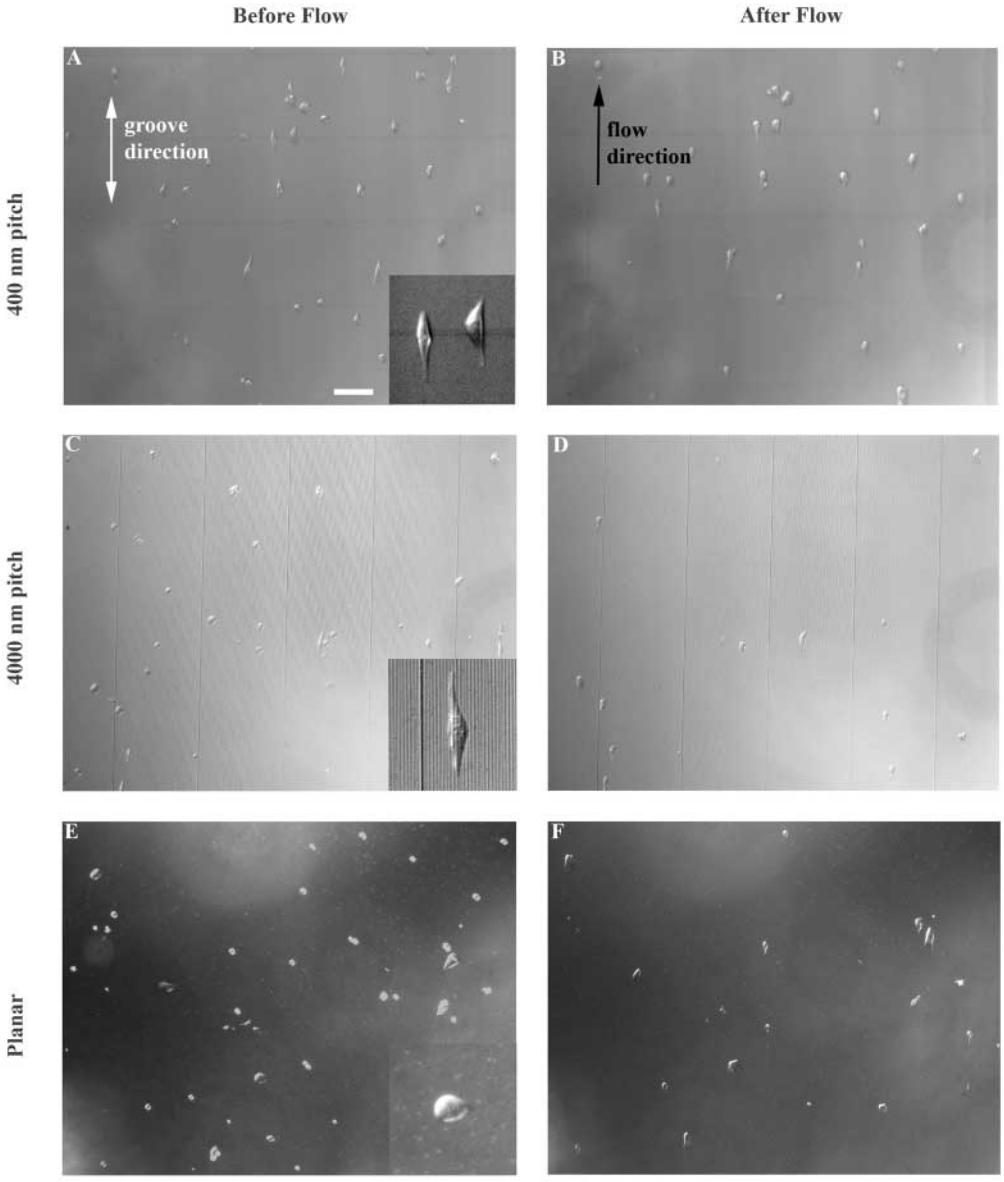

Fig. 4. Images of SV40-HCECs on the patterned and planar surfaces prior to and after exposure to uniform fluid shear. *Before Shear:* (A) 400 nm pitch, (C) 4000 nm pitch (E) planar surface. Insets in A, C and E show typical cell morphology on these surfaces. *AfterFlow* (maximum wall shear stress of 80 Pa): (B) 400 nm pitch, (D) 4000 nm pitch, (F) planar surface. Scale bar: 100 μm.

for 15 minutes (Fig. 5B). A comparison of cell detachment on the planar (data not shown) and the patterned surfaces (Fig. 5C) indicated that the response of primary cells to topography is similar to that of the SV40-HCECs. The trends in cell attachment shown in Fig. 5 were observed for each substratum, demonstrating that the smaller topographic features led to an increased ability of cells to adhere to the substratum.

Preliminary experiments indicated that the directionality of the flow with respect to the main axis of the patterns did not influence the experimental outcome (data not shown). In addition, a statistical analysis of the interaction effect between topography and fluid shear as determined by a 2-way ANOVA was not significant at the 95% level ($P<0.7$). The model equations used to calculate the wall shear stresses are based on the no-slip boundary condition, which means that the fluid at the solid surface has no velocity (Bird et al., 1960). The critical shear stress and shear rate at which the no-slip boundary condition fails to apply has been observed to increase exponentially with increasing surface roughness (Granick et al., 2003). Using the guidelines outlined by Stroock and co-workers, we calculated the effect of the patterns on the no-slip boundary conditions (Stroock et al., 2002). The slip velocity for flow parallel and perpendicular to the grooves was 5.10×10^{-2}–7.53×10^{-2} m/second and 2.55×10^{-2}–3.77×10^{-2} m/second, respectively. These values were considered negligible in modulating the wall shear stress (they accounted for a difference of 0.21-0.41% from the no-slip wall shear stress) and are in agreement with our experimental observation that the orientation of the main axis of the patterns relative to the direction of fluid flow had no significant influence in modulating the flow conditions. In subsequent experiments flow was directed parallel to the grooves because of chamber and substratum design specifications.

By sequentially imaging individual cells, we observed the dynamics of cell deformation in response to the applied shear force (Fig. 6). Cells on planar surfaces were mostly round

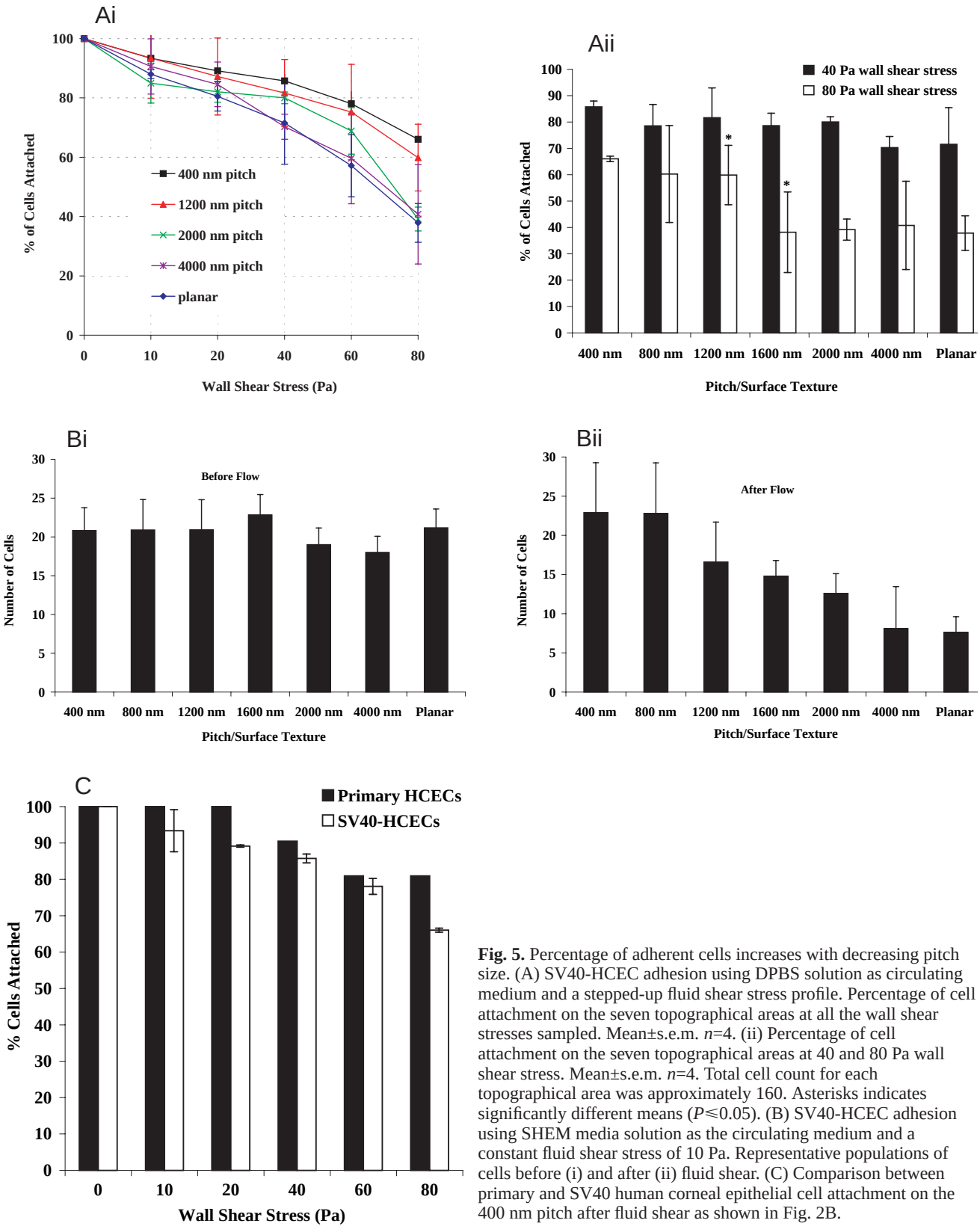

Fig. 5. Percentage of adherent cells increases with decreasing pitch size. (A) SV40-HCEC adhesion using DPBS solution as circulating medium and a stepped-up fluid shear stress profile. Percentage of cell attachment on the seven topographical areas at all the wall shear stresses sampled. Mean±s.e.m. n=4. (ii) Percentage of cell attachment on the seven topographical areas at 40 and 80 Pa wall shear stress. Mean±s.e.m. n=4. Total cell count for each topographical area was approximately 160. Asterisks indicates significantly different means ($P \leqslant 0.05$). (B) SV40-HCEC adhesion using SHEM media solution as the circulating medium and a constant fluid shear stress of 10 Pa. Representative populations of cells before (i) and after (ii) fluid shear. (C) Comparison between primary and SV40 human corneal epithelial cell attachment on the 400 nm pitch after fluid shear as shown in Fig. 2B.

before flow (Fig. 6A) and assumed a teardrop outline after flow (Fig. 6B-E). For planar surfaces a larger drop in the number of adherent cells was observed at a wall shear stresses of 40 Pa (Fig. 6D). The cells on the 400 nm pitch that were elongated before flow (Fig. 6F) were more resilient to the applied fluid shear (Fig. 6I,J). At wall shear stresses equal to and greater than 40 Pa, the cells on the 400 nm pitch were observed to assume a globular shape. In addition to displaying a similar

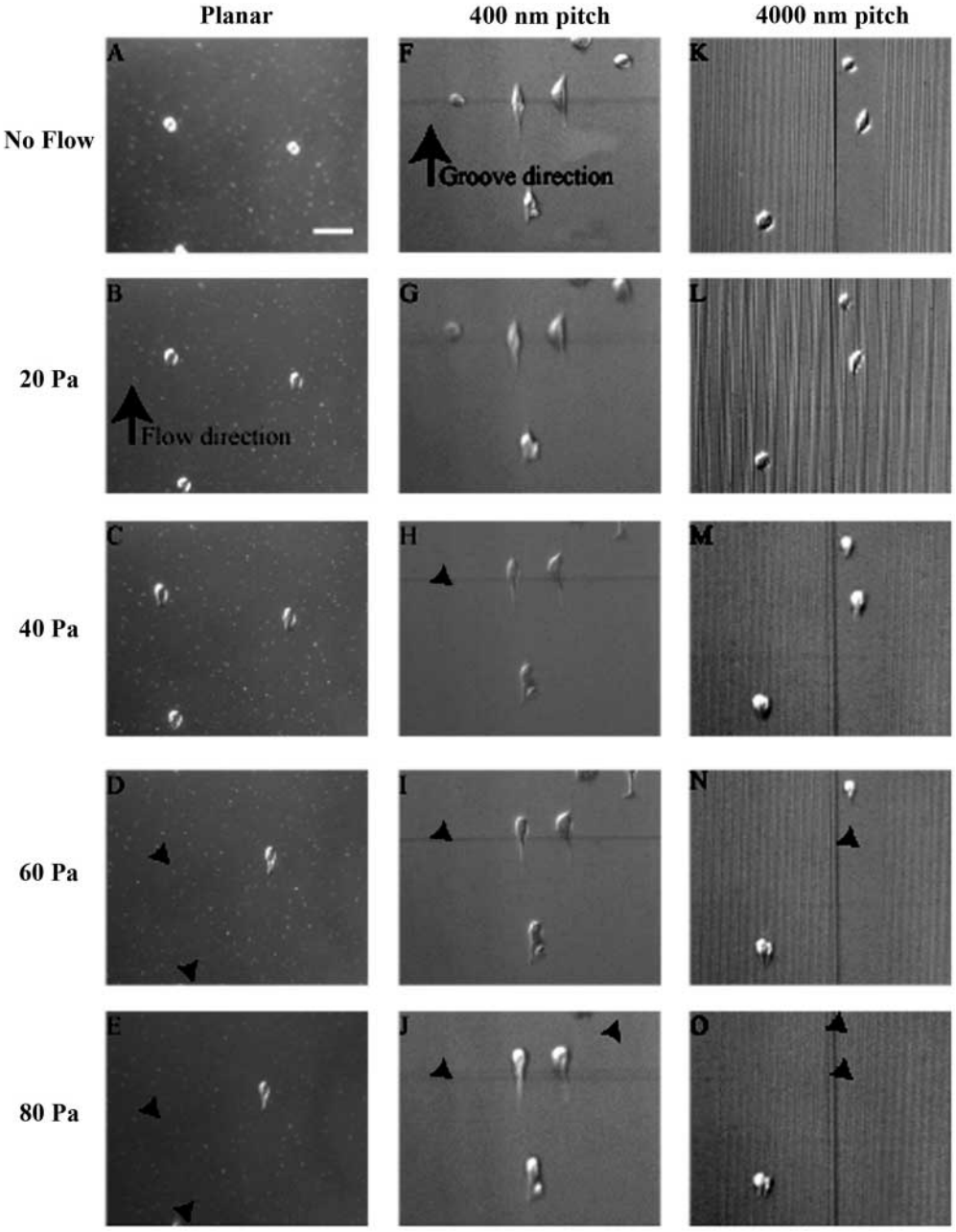

Fig. 6. Time-lapse images of cells on the 400 nm pitch, 4000 nm pitch and planar surface as they experience fluid shear stress: (A,F,K) No Flow (static conditions). (B-O) Wall shear stress of 20 Pa (B,G,L), 40 Pa (C,H,M), 60 Pa (D,I,N), 80 Pa (E,J,O). Arrowheads indicate position of detached cells. Scale bar: 50 μm.

detachment profile to the planar surface, cells on the 4000 nm pitch (Fig. 6L-P), including the elongated ones, also developed a tear drop morphology after the onset of flow. To investigate the possible relationship between elongation and cell adhesion we quantified the number of aligned and elongated cells before and after flow.

Analysis of our results indicated that the percentage of aligned and elongated cells decreased considerably after flow on both the nano- and microscale patterned substrata (Fig. 7). Prior to flow, 40% and 33% of the cells were aligned parallel to the grooves on the 400 nm and 4000 nm pitch surfaces, respectively. After a systematic increase in wall shear (Fig. 2B), the percentage of aligned and elongated cells decreased to 4.2% and 7.3% of the original cell population for the 400 nm and 4000 nm pitch, respectively. The data seem to be compatible with two distinct scenarios. The first is that aligned cells are less adhesive than non-aligned cells and hence easier to detach. The second is that aligned cells become more unaligned. Sequential imaging of the cells (Fig. 6) demonstrated that aligned cells seem to loose their alignment under high fluid shear on the 400 nm pitch but were more adhesive than cells that were not aligned prior to the onset of flow. On large feature sizes (the 4000 nm pitch) alignment did not correlate with adhesiveness.

Discussion

Previous studies over the past two decades have suggested that the underlying substratum topography influences cell behaviors including proliferation, migration, and adhesion by

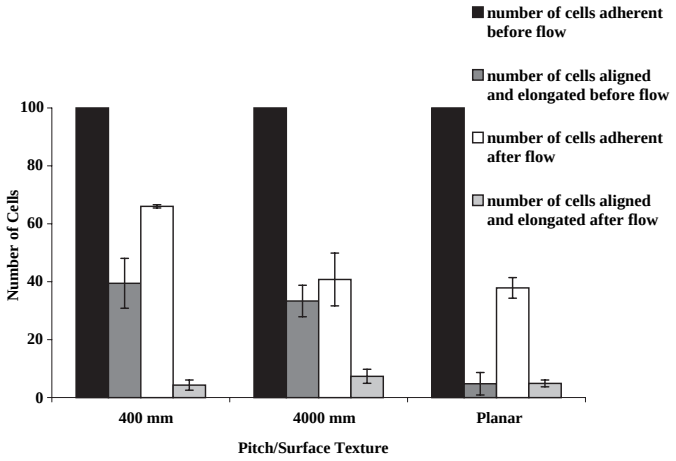

Fig. 7. Populations of oriented and elongated cells before and after flow and the number of cells still adherent at maximum wall shear stress. The numbers are based on 100 adherent cells before flow. The total number of cells analyzed was approximately 200 for each type of topography sampled. Mean±s.e.m. *n*=4.

both direct and indirect interactions (Abrams et al., 2002b; Brunette, 1986a; Brunette, 1986b; Brunette and Chehroudi, 1999; Curtis and Wilkinson, 1998; Evans et al., 1999b; Ingber, 1997; Meier and Hay, 1975; Oakley and Brunette, 1995; Teixeira et al., 2003; Wojciak-Stothard et al., 1996; Wojciak-Stothard et al., 1995). Corneal epithelial cells interact with a complex basement membrane composed of proteoglycans, collagen fibers and multi-adhesive matrix proteins which form a rich three-dimensional structure with characteristic nanoscale dimensions (Abrams et al., 2002a; Abrams et al., 2000a; Abrams et al., 2000b). In order to elucidate how corneal epithelial cells are influenced by the underlying topography, we applied a biologically relevant model system to examine cell-substratum adhesion. We hypothesized that topography with nanoscale dimensions, which closely approximate the size of in vivo topographical features found in the native basement membrane, would better support epithelial cell attachment as compared to planar surfaces or surfaces with microscale dimensions.

We fabricated silicon surfaces with uniform groove and ridge patterns with dimensions ranging from 400-4000 nm pitch using X-ray lithography. Light and scanning electron microscopy of corneal epithelial cells showed that prior to flow approximately one third of the cell population was aligned and oriented in the direction of the grooves and that cell-substratum contact was restricted to the tops of the ridges for all feature sizes. Our findings are similar to those reported by Teixeira and co-workers, where up to 35% of primary HCECs were found to orient in the direction of the groove ridge with the same pitch dimensions as those used in the present study (Teixeira et al., 2003). Teixeira and co-workers reported that 11% of primary HCECs oriented in a preferred direction on the planar surfaces while we found that approximately 5% of SV40-HCECs orient and elongate in a preferred direction on the planar surfaces. The difference in percentages between our study and that by Teixeira and co-workers is that they isolated orientation and elongation from one another while we have used both as a measure of cell morphology. Subsequently, our findings reinforce the perception that orientation and elongation are coupled morphological changes for cells on patterned surfaces. Teixera and co-workers also observed that cell-substratum adhesion was restricted to the tops of the ridges and that filopodia in primary HCECs adhered to the grooves and ridges of patterns for all pattern dimensions. Evans and co-workers, found that basement membrane and hemidesmosomal plaque components in epithelial tissue were restricted to the areas between the pores for pore sizes 400-2000 nm thereby restricting cell-substratum contacts to the regions between the pores (Evans et al., 1999b). Other investigators have reported cell alignment and elongation for different cell types on microscale grooves. Evans and co-workers observed that fetal and neonatal myoblasts aligned parallel with the direction of 2.3-6.0 micron deep grooves (Evans et al., 1999a). Brunette and co-workers found alignment, elongation and migration of epithelial cells parallel to v-shaped microgrooves (Brunette, 1986b). They also reported an increase in alignment and locomotion with increasing groove depth. In addition, rat dermal fibroblasts (den Braber et al., 1996), central nervous system neurites (Rajnicek and McCaig, 1997) and baby hamster kidney cells (Britland et al., 1996) have also been reported to align and elongate parallel to the long axis of micron scale grooves.

In support of our findings, Teixeira and co-workers also found no change in primary HCEC alignment for the pitch dimensions of 400 to 4000 nm but observed an increase in cell alignment with increases in groove depth (Teixeira et al., 2003). In our experiments we found groove depth between patterned regions to vary by 150 nm. The greatest depth was associated with the largest patterns (4000 nm pitch). It would be expected, for these surfaces, that experimental conditions would favor finding a more positive effect for largest feature size. This was not observed, adding to the robustness of our findings.

Biological functions of adherent cells are partly regulated through cell shape and deformability. The physical state of the ECM has been reported to affect the cell shape. Huang and Ingber demonstrated that the control of cell shape using fabricated substrata coated with fibronectin led to controlled cell cycle progression (Huang et al., 1998). Streuli demonstrated that mammary gland epithelial cells in vitro that adopted a cuboidal morphology expressed higher levels of β-casein than cells that were induced to spread out (Streuli et al., 1991). Chen and co-workers demonstrated a relationship between cell cycle progression, cell-ECM contact area and cell spreading on micropatterned substrata (Chen et al., 1997). It has been proposed that since the ECM physically connects with the cytoskeleton, its mechanical properties may contribute significantly to the mechanotransduction response (Ingber, 1997). Therefore, the physical state of the ECM affects cell shape and may subsequently determine changes in adhesion. The ECM components deposited by the overlying cells take on the physical form of the substrata and this may provide the physical stimulus that is needed to change cell morphology and associated events such cell-substratum interactions. We measured the adhesive strength of HCECs while simulating the mechanical forces they are subjected to in vivo by challenging the adherent cells to a well defined fluid shear and monitoring the number of adherent cells as a function of wall shear stress.

In our analyses we considered that cell detachment was

primarily due to the failure of cell-substratum interactions and not to cohesive failure (Richards et al., 1995). This is supported by the fact that we did not observe any cell debris or 'ghost cells', which are associated with cell rupture, during the course of our adhesion assays. Cohesive failure occurs when shear forces are greater than the cohesive strength of the cell. The fact that we observed the same adhesive response with respect to substratum topography using a stepped up fluid shear stress and a low constant fluid shear stress seems to indicate that the primary action of the applied force was to cause failure in cell-substratum interactions. Furthermore, human corneal epithelial cells in vivo are exposed to shear stresses that are approximately three times greater than the maximum shear stress used in our experiments, without cell rupture occurring (King-Smith et al., 2000; Fatt, 1992). While we did not explore the precise nature of the cohesive strength of HCECs, we deduce that it is much larger than the forces applied in our experiments. We therefore feel it reasonable to assume that the main action of the applied force was to disrupt cell-substratum contacts.

The increase in the number of adherent cells on the 400 nm pitch pattern, as compared to the planar surface and the patterns with 800-4000 nm pitches supports our hypothesis that cells would adhere better on a substratum that had features that more closely approximate the native corneal basement membrane. A clear biphasic trend was observed, with increased cell adhesion on smaller feature sizes. Our statistical analysis showed significant differences between the 400 nm pitch and the 4000 nm pitch patterns and between the 400 nm pitch pattern and the planar surface. Adhesion of HCECs on the 4000 nm pitch was statistically indistinguishable from adhesion on the planar surfaces.

In support of our findings, Evans and co-workers also found differences in adhesion when groups of cells were plated on nanoscale features as compared to microscale features (Evans et al., 1999b). Their investigation on epithelial tissue adhesion to porous polycarbonate surfaces revealed that confluent cells on the smallest pore size, 100 nm pores, had the highest number of hemidesmosomes. In addition, cells plated on surfaces with microscale pores were unable to form or had very few hemidesmosomes. This study and a subsequent study on the effect of pore density used sheets of epithelial cells (Evans et al., 1999b; Evans et al., 2003) and found that cell-cell signaling influences cell behavior. Our study, in contrast, was focused on individual cells. Nonetheless, the results we have obtained for single cells are interesting in that they may be relevant to how the behavior of individual cells relates to the behavior observed in confluent cells.

It has recently been reported that the highest cell attachment in rat epitenon fibroblast cells is at the groove ridge transitions (Curtis et al., 2001). The discontinuities on our patterned surfaces may contribute to increased adhesion by providing more available binding sites that ensure favorable cell-substratum adhesion protein conformations. Using SEM image analysis the number of discontinuities a cell interfaces with on the 400 nm pattern is 74 and on a 4000 nm pitch pattern is nine (Fig. 8). The smaller the pitch, the greater the numbers of groove/ridge transitions that are in contact with the cells and subsequently, the stronger the attachment.

In assessing the results from our adhesion assay, we assumed that the only physical stimuli that cells received were from the

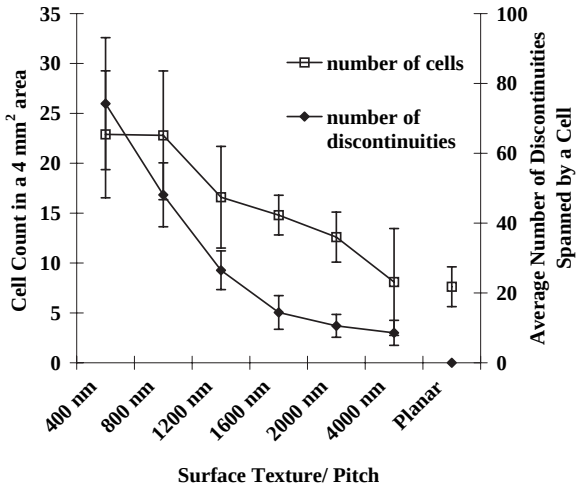

Fig. 8. The effect of surface discontinuities on cell adhesion on the different feature sizes. Both the average number of discontinuities that a cell interfaced and the number of adherent cells present after exposure to a wall shear stress of 10 Pa for 15 minutes are presented as a functions of surface topography. The number of surface discontinuities that a cell spanned was determined from SEM images of cells on the different topographical areas. For SEM analysis the total number of cells examined was 25. Mean±s.e.m. $4 \leqslant n \leqslant 7$.

topography. It is possible that within the time frame of the adhesion assays, fluid shear stress and topography were acting in concert to modulate cell adhesion. Corneal epithelial cells in their natural environment are constantly under fluid shear and it is possible that fluid shear enhances cell-substratum adhesion. Qualitative analyses of images taken during flow demonstrated changes in cell morphology. It is possible that shear stress was not only causing the failure of cell-substratum interactions but may have been causing a reorganization of the cellular cytoskeleton on the patterned surfaces. These changes may enhance the ability of the cells to withstand fluid shear. The time lapse images demonstrated that the aligned and elongated cells on the 400 nm pitch had a greater ability to withstand fluid shear. The adhesive interactions of the elongated and aligned cells on the 4000 nm pitches were not stable and were seen to fail easily, resulting in cell detachment of both the round and elongated cells.

F-actin protein labeling, after flow, demonstrated a significant decrease in the number of aligned and elongated cells on both the 400 and the 4000 nm pitch patterns after flow. While, it may be possible that cellular reaction to the applied shear stress in the elongated and aligned cells on the 400 nm pitches is to spread perpendicularly to the grooves we were not able to detect this through our time-lapse images. We propose that the shearing action of the fluid is causing the rupture of cell-substratum linkages that are responsible for aligning and elongating the HCECs on the 400 nm pitch without entirely shearing the cells off. This is possibly due to the strong cell-substratum interactions on the nanoscale patterns. Conversely, the cells on the 4000 nm pitch have weaker adhesive interactions and are easily sheared off regardless of cell morphology.

In spite of our finding that there is no statistically significant interaction between topography and fluid shear we cannot totally discount the mechanotransduction effect of fluid flow

on the strength of adhesion to our substrata. Davies and co-workers demonstrated that the application of fluid stress to the apical membrane of vascular endothelial cells resulted in the cytoskeleton being pulled against its fixed basal contacts resulting in dynamic changes in focal adhesion complex remodeling at the base of the cell, which occurred within seconds to minutes after shear was exerted (Davies et al., 1994). Teixeira and co-workers observed that the width of focal adhesions formed on substrata similar to those used in this study depended on the ridge size (Teixeira et al., 2003). It is possible that there is remodeling of focal adhesions on our patterned substrata in response to flow, which may be reflected in the ability of the cell to withstand fluid shear. Future work will examine dynamic changes within the cell cytoskeleton and focal adhesion assembly as a function of fluid shear and topography.

In conclusion, our study demonstrated that the adhesive strength of HCECs is significantly modulated by substratum topography. Cell contact on patterns with uniform grooves and ridges ranging from nano- to microscale was observed to be restricted to the tops of the ridges and the cell thickness was constant on the different topographies. Furthermore, we demonstrated a biphasic adhesive cellular response with regards to substratum topography with a transition point occurring at the 1200-1600 nm pitch that marked the difference between nano- and microscale adhesive response. Cells were more adherent on the nanoscale or biological length scale topographic features. We suspect that this response may be attributed to the discontinuities interfaced by the adherent cells. This finding is novel in that it is the first study that clearly quantifies the strength of cell-substratum adhesion on synthetic nano- and micro-scale topographies by using a biologically relevant challenge. Our findings have relevance to the interpretation of in vitro data as well as to the study of cellular interactions with biomaterials. Future work will be targeted at exploring the mechanisms of action that lead to enhanced cell-substratum binding on the nanoscale topographic features.

This work was supported by grants from the National Eye Institute (RO1 EY 012253-01) and NSF MRSEC (DMR-9632527). N.W.K. gratefully acknowledges the contribution of Stella Wanjugu Karuri in the statistical analysis of the experimental data. Facilities at the Center for Nanotechnology at the University of Wisconsin-Madison are supported in part by DARPA/ONR grant number N00014-97-1-0460. The authors thank the Wisconsin and Missouri Lions Eye Banks for providing corneas.

References

Abrams, G. A., Goodman, S. L., Nealey, P. F., Franco, M. and Murphy, C. J. (2000a). Nanoscale topography of the basement membrane underlying the corneal epithelium of the rhesus macaque. *Cell Tissue Res.* **299**, 39-46.

Abrams, G. A., Schaus, S. S., Goodman, S. L., Nealey, P. F. and Murphy, C. J. (2000b). Nanoscale topography of the corneal epithelial basement membrane and descemet's membrane of the human. *Cornea* **19**, 57-64.

Abrams, G. A., Bentley, E., Nealey, P. F. and Murphy, C. J. (2002a). Electron microscopy of the canine corneal basement membranes. *Cells Tissues Organs* **170**, 251-257.

Abrams, G. A., Teixeira, A. I., Nealey, P. F. and Murphy, C. J. (2002b). Effects of substratum topography on cell behavior. In *Biomimetic Materials and Design* (ed. A. K. Dillow and A. M. Lowman), pp. 91-137. New York, NY: Marcell Dekker.

Araki-Sasaki, K., Ohashi, Y., Sasabe, T., Hayashi, K., Watanabe, H., Tano, Y. and Handa, H. (1995). An SV40-immortalized human corneal epithelial cell line and its characterization. *Invest. Ophthalmol. Vis. Sci.* **36**, 614-621.

Bird, R. B., Stewart, W. E. and Lightfoot, E. N. (1960). Velocity distributions in laminar flow. In *Transport Phenomena*, p. 62. New York, NY: Wiley.

Britland, S., Morgan, H., Wojiak-Stodart, B., Riehle, M., Curtis, A. and Wilkinson, C. (1996). Synergistic and hierarchical adhesive and topographic guidance of BHK cells. *Exp. Cell Res.* **228**, 313-325.

Brunette, D. M. (1986a). Fibroblasts on micromachined substrata orient hierarchically to grooves of different dimensions. *Exp. Cell Res.* **164**, 11-26.

Brunette, D. M. (1986b). Spreading and orientation of epithelial cells on grooved substrata. *Exp. Cell Res.* **167**, 203-217.

Brunette, D. M. and Chehroudi, B. (1999). The effects of the surface topography of micromachined titanium substrata on cell behavior in vitro and in vivo. *J. Biomech. Eng.* **121**, 49-57.

Chen, C. S., Mrksich, M., Huang, S., Whitesides, G. M. and Ingber, D. E. (1997). Geometric control of cell life and death. *Science* **276**, 1425-1428.

Chou, L., Firth, J. D., Uitto, V. J. and Brunette, D. M. (1995). Substratum surface topography alters cell shape and regulates fibronectin mRNA level, mRNA stability, secretion and assembly in human fibroblasts. *J. Cell Sci.* **108**, 1563-1573.

Curtis, A. S. and Wilkinson, C. D. (1997). Topographical control of cells. *Biomaterials* **18**, 1573-1583.

Curtis, A. S. and Wilkinson, C. D. (1998). Reactions of cells to topography. *J. Biomater. Sci.* **9**, 1313-1329.

Curtis, A. S., Casey, B., Gallagher, J. O., Pasqui, D., Wood, M. A. and Wilkinson, C. D. (2001). Substratum nanotopography and the adhesion of biological cells. Are symmetry or regularity of nanotopography important? *Biophys. Chem.* **94**, 275-283.

Davies, P. F., Robotewskyj, A. and Griem, M. L. (1994). Quantitative studies of endothelial cell adhesion. Directional remodeling of focal adhesion sites in response to flow forces. *J. Clin. Invest.* **93**, 2031-2038.

den Braber, E. T., de Ruijter, J. E., Smits, H. T., Ginsel, L. A., von Recum, A. F. and Jansen, J. A. (1996). Quantitative analysis of cell proliferation and orientation on substrata with uniform parallel surface micro-grooves. *Biomaterials* **17**, 1093-1099.

Evans, D. J., Britland, S. and Wigmore, P. M. (1999a). Differential response of fetal and neonatal myoblasts to topographical guidance cues in vitro. *Dev. Genes Evol.* **209**, 438-442.

Evans, M. D., Dalton, B. A. and Steele, J. G. (1999b). Persistent adhesion of epithelial tissue is sensitive to polymer topography. *J. Biomed. Mater. Res.* **46**, 485-493.

Evans, M. D., Taylor, S., Dalton, B. A. and Lohmann, D. (2003). Polymer design for corneal epithelial tissue adhesion: pore density. *J. Biomed. Mater. Res.* **64**, 357-364.

King-Smith, P. E., Fink, B. A., Fogt, N., Nichols, K. K., Hill, R. M. and Wilson, G. (2000). The thickness of the human precorneal tear film: evidence from reflection spectra. *Invest. Ophthalmol. Vis. Sci.* **41**, 3348-3359.

Fatt, I. (1992). Architecture of the lid-cornea juncture. *CLAO J.* **18**, 187-192.

Flemming, R. G., Murphy, C. J., Abrams, G. A., Goodman, S. L. and Nealey, P. F. (1999). Effects of synthetic micro- and nano-structured surfaces on cell behavior. *Biomaterials* **20**, 573-588.

Granick, S., Zhu, Y. and Lee, H. (2003). Slippery questions about complex fluids flowing past solids. *Nat. Mater.* **2**, 221-227.

Huang, S., Chen, C. S. and Ingber, D. E. (1998). Control of cyclin D1, p27(Kip1), and cell cycle progression in human capillary endothelial cells by cell shape and cytoskeletal tension. *Mol. Biol. Cell* **9**, 3179-3193.

Ingber, D. E. (1997). Tensegrity: the architectural basis of cellular mechanotransduction. *Annu. Rev. Physiol.* **59**, 575-599.

Meier, L. and Hay, E. D. (1975). Stimulation of corneal differentiation by interaction between cell surface and extracellular matrix. I. Morphometric analysis of transfilter "induction". *J. Cell Biol.* **66**, 275-291.

Oakley, C. and Brunette, D. M. (1995). Response of single, pairs, and clusters of epithelial cells to substratum topography. *Biochem. Cell Biol.* **73**, 473-489.

Rajnicek, A. and McCaig, C. (1997). Guidance of CNS growth cones by substratum grooves and ridges: effects of inhibitors of the cytoskeleton, calcium channels and signal transduction pathways. *J. Cell Sci.* **110**, 2915-2924.

Rajnicek, A., Britland, S. and McCaig, C. (1997). Contact guidance of CNS neurites on grooved quartz: influence of groove dimensions, neuronal age and cell type. *J. Cell Sci.* **110**, 2905-2913.

Richards, R. G., Gwynn, I., Bundy, K. J. and Rahn, B. A. (1995). Microjet impingement followed by scanning electron microscopy as a qualitative technique to compare cellular adhesion to various biomaterials. *Cell Biol. Int. Rep.* **19**, 1015-1024.

Streuli, C. H., Bailey, N. and Bissell, M. J. (1991). Control of mammary epithelial differentiation: basement membrane induces tissue-specific gene expression in the absence of cell-cell interaction and morphological polarity. *J. Cell Biol.* **115**, 1383-1395.

Stroock, A. D., Dertinger, S. K., Whitesides, G. M. and Ajdari, A. (2002). Patterning flows using grooved surfaces. *Anal. Chem.* **74**, 5306-5312.

Teixeira, A. I., Abrams, G. A., Bertics, P. J., Murphy, C. J. and Nealey, P. F. (2003). Epithelial contact guidance on well-defined micro- and nanostructured substrates. *J. Cell Sci.* **116**, 1881-1892.

Timpl, R. (1996). Macromolecular organization of basement membranes. *Curr. Opin. Cell Biol.* **8**, 618-624.

Timpl, R. (1989). Structure and biological activity of basement membrane proteins. *Eur. J. Biochem.* **180**, 487-502.

Wojiak-Stodart, B., Curtis, A. S., Monaghan, W., McGrath, M., Sommer, I. and Wilkinson, C. D. (1995). Role of the cytoskeleton in the reaction of fibroblasts to multiple grooved substrata. *Cell Motil. Cytoskeleton* **31**, 147-158.

Wojciak-Stothard, B., Curtis, A., Monaghan, W., MacDonald, K. and Wilkinson, C. (1996). Guidance and activation of murine macrophages by nanometric scale topography. *Exp. Cell Res.* **223**, 426-435.

Woods, A. and Couchman, J. R. (1988). Focal adhesions and cell-matrix interactions. *Coll. Relat. Res.* **8**, 155-182.